Scientific Research Publishing

American Journal of Analytical Chemistry, 2018, 9, 311-321
http://www.scirp.org/journal/ajac
ISSN Online: 2156-8278
ISSN Print: 2156-8251

Comparison of the Vibrational Spectra of Copper Polysilicate, $CuSiO_3$, with Those of the Prototypic Copper Polygermanate, $CuGeO_3$

Marco Meibohm, Hans Hermann Otto*

Materials Science and Crystallography, Technical University of Clausthal, Clausthal-Zellerfeld, Lower Saxony, Germany
Email: *hhermann.otto@web.de

How to cite this paper: Meibohm, M. and Otto, H.H. (2018) Comparison of the Vibrational Spectra of Copper Polysilicate, $CuSiO_3$, with Those of the Prototypic Copper Polygermanate, $CuGeO_3$. *American Journal of Analytical Chemistry*, **9**, 311-321.
https://doi.org/10.4236/ajac.2018.96024

Received: March 5, 2018
Accepted: June 4, 2018
Published: June 7, 2018

Abstract

Orthorhombic copper polysilicate, $CuSiO_3$, is isotypic to the spin-Peierls compound $CuGeO_3$ and represents a further example of a quasi-one-dimensional spin = 1/2 antiferromagnetic *Heisenberg* chain system. This is a representation of the first Raman and IR/FIR spectra for $CuSiO_3$, measured at room temperature on polycrystalline samples. A comparison of the optical phonons, predicted by a factor group analysis, with those observed for the $CuGeO_3$ prototype, is presented. A mode assignment for the silicate is given. Surface effects due to a very small crystallite size may cause additional broad bands observed in the Raman spectrum of $CuSiO_3$. From the analysis of the *Davydov* doublet an intralayer-to-interlayer bond strength of about 40 is derived for the silicate, which is about 20% lower than for the isotypic germanate, allowing for different magnetic responses at low temperature.

Keywords

IR/FIR Spectra, Raman Spectra, Factor Group Analysis, Davydov Analysis, Copper Polysilicate, $CuSiO_3$, Copper Polygermanate, $CuGeO_3$, Low-Dimensional Compounds, Spin-Peierls Transition

1. Introduction

Low-dimensional quantum spin systems are of considerable theoretical and experimental interest. Some years ago a spin dimerization transition (spin-Peierls transition), which is one of the quantum phenomena in a S = 1/2 antiferromagnetic *Heisenberg* linear chain, was observed in inorganic compounds and extensively studied in quasi-one-dimensional (1D) copper polygermanate, $CuGeO_3$ [1] [2] respectively α' – NaV_2O_5 [3].

The crystal structure of copper polygermanate consists of two types of chains which running down the shortest translation period: *einer* single chains of GeO_4 tetrahedra are connected by chains of edge-sharing CuO_{4+2} "octahedra" [4] [5], which are in reality due to the *Jahn-Teller* effect strongly elongated and distorted tetragonal dipyramids. Because of this the magnetic chains actually are formed by ladders of CuO_2 squares.

Until now $CuGeO_3$ was the prototypic compound showing such tetrahedral single chains with a repeat sequence of only one GeO_4 unit. The substitution of Si^{4+} for Ge^{4+} in copper polygermanate according to $CuGe_{1-x}Si_xO_3$ was only possible in the limited concentration range $x \leq 0.5$ for polycrystals by hydrothermal synthesis [6], and the existence of pure $CuSiO_3$ was considered non-existent [7] [8]. However, we succeeded in the preparation of polycrystalline $CuSiO_3$, isotypic to $CuGeO_3$, by thermal decomposition of the mineral dioptase, $Cu_6Si_6O_{18}\cdot 6H_2O$, and investigated its crystal and magnetic structure [9] [10] [11] [12]. Strong bonds in the *ac*-plane form zigzag layers in the crystal structure (**Figure 1**), but the layer-like character is less pronounced for the silicate than for the germanate, because its interlayer distance is reduced about 3.6% and the intralayer chain distance enlarged about 3.5% in comparison to the germanate. Lattice parameters and CuO_2 chain separations of both compounds are compared in **Table 1** and individual bond lengths summarized in **Table 2** to complete the data used for the further analysis [10] [13].

Here we report on a first investigation of the room temperature vibrational spectra of a polycrystalline $CuSiO_3$ sample and compare these measurements with that for $CuGeO_3$ using previously reported data as well as our own. While the synthesis of $CuGeO_3$ can easily be performed as a polycrystalline powder by sintering of equimolar amounts of CuO and GeO_2 at 800˚C [11], or as single crystals by the floating zone method [14], the synthesis of pure $CuSiO_3$ remains a worthwhile task. This paper is an extended (and corrected) version of a contribution that has been pre-published some years ago [15].

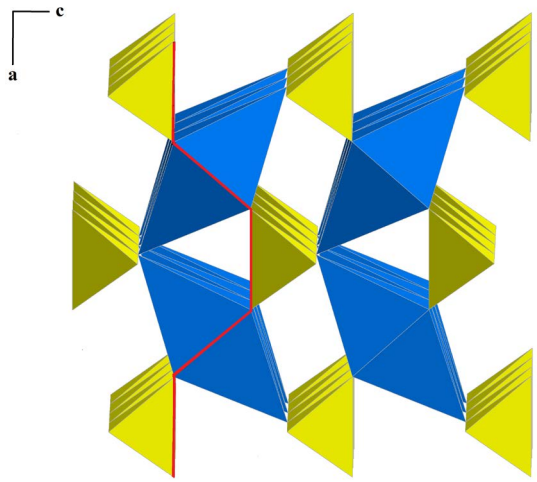

Figure 1. Crystal structure projection of $CuSiO_3$ along [010]. Zigzag layers along *a* in the *ac* plane are depicted by the red line.

Table 1. Lattice parameters, unit-cell volume and separations of CuO_2 chains for isotypic $CuSiO_3$ [10] [11] [12] and $CuGeO_3$ [13], respectively. Space group *Pmma* (No. 51, standard setting).

Compound	*a* (Å)	*b* (Å)	*c* (Å)	*V* (Å^3)
$CuSiO_3$	8.7735 (11)	2.8334 (4)	4.6357 (6)	115.24 (5)
$CuGeO_3$	8.4749 (3)	2.9431 (1)	4.8023 (2)	119.78 (2)
	CuO_2 chain separations in the unit cell			
	***a*/2 (Å)** intralayer		***c* (Å)** interlayer	
$CuSiO_3$	4.3868 (5)		4.6357 (6)	
$CuGeO_3$	4.2375 (2)		4.8023 (2)	

Table 2. Bond lengths for $CuSiO_3$ and $CuGeO_3$.

Compound	Atoms	Bond length (Å)	Reference
$CuSiO_3$	Cu – O (1)	2.926 (7) *x* 2	[10]
	Cu – O (2)	1.941 (4) *x* 4	
	Si – O (1)	1.640 (7) *x* 2	
	Si – O (2)	1.582 (7) *x* 2	
$CuGeO_3$	Cu – O (1)	2.7549 (8) *x* 2	[13]
	Cu – O (2)	1.9326 (7) *x* 4	
	Ge – O (1)	1.7730 (8) *x* 2	
	Ge – O (2)	1.7322 (10) *x* 2	

2. Experimental

The Raman and IR spectra of $CuSiO_3$ and $CuGeO_3$ were measured on polycrystalline samples. The copper polysilicate specimen has been obtained by thermal decomposition of the mineral dioptase, $Cu_6Si_6O_{18}{\cdot}6H_2O$, as a multi-phase educt containing about 76 wt-% $CuSiO_3$, 14 wt-% CuO (tenorite) and 10 wt-% amorphous SiO_2 [10]. Single-phase powder of $CuGeO_3$ has been synthesized by sintering of pellets of a thoroughly homogenized CuO and GeO_2 mixture at 1200 K and a repeated grinding and sintering procedure.

The Raman spectrum of $CuSiO_3$ was recorded with a *DILOR LabRAM* spectrometer, using a Nd-YAG-laser with frequency doubler (λ = 532 nm) as an exciting source, and the spectrum of $CuGeO_3$ with a Raman FRA 106 modul attached to a *BRUKER IFS* 66v interferometer, using once again a Nd-YAG-laser, but with λ = 1064 nm. Infrared spectra of both compounds were obtained with the above mentioned interferometer using CsI pellets of the powdered samples.

The IR and Raman spectra of the minor phases in the phase mixture (CuO as tenorite and amorphous SiO_2) were also recorded with the same experimental equipment in order to estimate the possible distortion of the $CuSiO_3$ spectra and are given by Meibohm (1999) [11]. Only few strong bands were observed (IR: 470 and 1108 cm^{-1} for amorphous SiO_2 and 530 cm^{-1} for CuO; Raman: 450 cm^{-1}

for amorphous SiO_2 and 300 cm^{-1} for CuO) that would be in a position to introduce a marginal distortion of the main phase spectra. Only the background of the Raman spectrum near 300 cm^{-1} as well as the left (high frequency) shoulder of the IR band near 500 cm^{-1} may be influenced by the presence of the minor phases.

3. Crystallographic Data

Relevant crystallographic data such as lattice parameters, bond lengths and chain separations are summarised in Table 1 and Table 2 for both $CuSiO_3$ and $CuGeO_3$. The Figures 1-3 illustrate crystal structural details in the standard setting (space group *Pmma*).

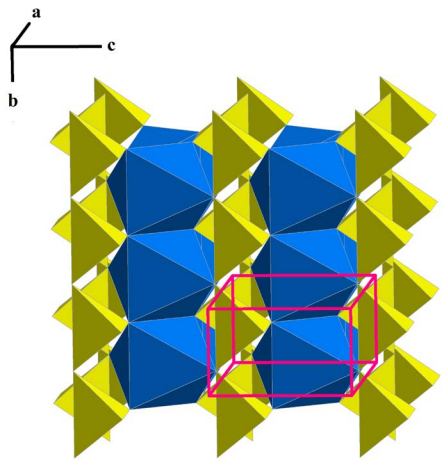

Figure 2. Polyhedral representation of the $CuSiO_3$ crystal structure. The unit cell was outlined in margenta color, silicate tetrahedral chains in yellow color, copper oxide octahedral chains in blue color, respectively.

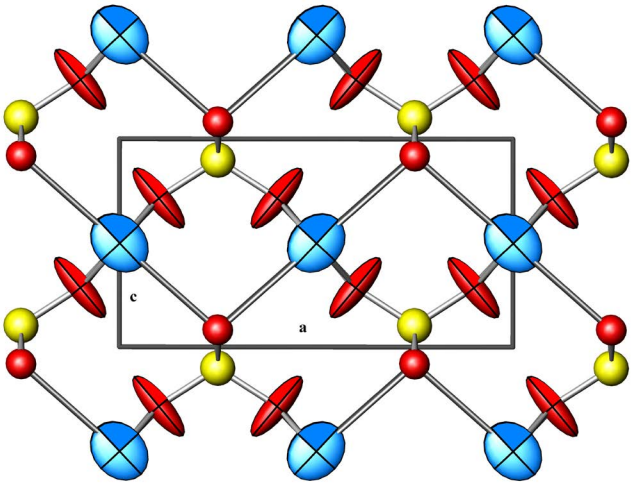

Figure 3. Projection of the crystal structure of $CuSiO_3$ along the *b*-axis in the displacement ellipsoid representation [12]. Oxygen atoms red, Cu atoms blue, Si atoms yellow, respectively. The strongly anisotropic displacement of the oxygen atom O(2) is noticeable.

4. Factor Group Analysis

For the factor group analysis (f.g.a.) the unit-cell, containing two non-translationally equivalent $CuSiO_3$ units and thus n = 10 atoms, were adapted to the standard setting of the Pmma space group in order to apply the tables given by Rousseau [16] and Adams [17] and to compare with the data already reported for $CuGeO_3$ [18]-[23]. From the total number of vibrations ($N_T = 3n = 30$) the 3 acoustic and 2 silent modes were subtracted, leaving 25 remaining optic modes, 12 of which are Raman-active and 13 IR-active modes. The results are summarized in **Figure 4** displaying the active modes in frames. The following are features of the analysis that will make the mode assignment easier: a) the copper atoms do not contribute to the Raman spectrum; b) coupling between the two non-translationally equivalent silicate chains of C_{2v} site symmetry in the unit-cell with D_{2h} symmetry leads to *Davydov* pairs [24]; the chain modes split into crystal modes of type $A_g - B_{1u}$, $B_{2g} - B_{3u}$ and $B_{3g} - B_{2u}$, respectively [19]. The obtained doublets involving both Raman- and IR-active modes are indicated in **Figure 4** by vertical lines.

5. Results and Discussion

The room temperature Raman and infrared spectra of both $CuSiO_3$ and $CuGeO_3$ are shown in **Figure 5** and **Figure 6**, and the extracted vibrational frequencies are summarized in **Table 3** along with their intensities and the mode assignments. At a rough estimate the spectra of the silicate shift on average by a factor of $F = F_{m^*} \cdot F_{bl} = 1.23$ to higher frequencies in comparison to that of the germanate. In this way the mode assignment for the germanate, confirmed by a normal coordinate analysis [13], can be applied to the silicate spectra. In particular is

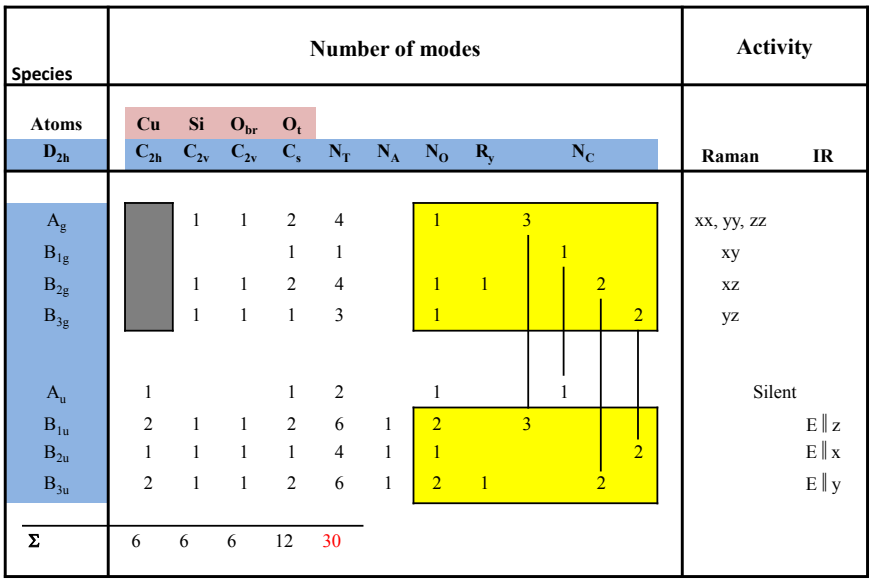

Figure 4. Factor group analysis for orthorhombic $CuSiO_3$ (space group D_{2h}–*Pmma*, No. 51). Mode numbers: N_T total number, N_A acoustic branch, N_O optic branch, R_y chain librations, N_C coupled vibrations of two chains, O_t = terminal oxygen atom, O_{br} = bridging oxygen atom.

Table 3. Vibrational frequencies (cm^{-1}) and mode assignment for $CuSiO_3$ and $CuGeO_3$.

$CuGeO_3$			Mode Assignment			$CuSiO_3$		
Raman		**IR**	**Raman**		**IR**	**Raman**		**IR**
880 w			B_{2g}			1019 w		
858 s	-	857 s	A_g	-	B_{1u}	998 m	-	1092 m
		776 vs			B_{3u}			959 s
712 w	-	718 vs	B_{3g}	-	B_{2u}	854 vw	-	859 vs
592 vs	-	619 m	A_g	-	B_{1u}	719 m	-	737 s
						634 m ?		
						590 m, b ?		
		528 vs			B_{2u}			576 vs
		478 m, sh			B_{1u}			558 m
430 vw	-	380 s	B_{2g}	-	B_{3u}	480 vw	-	465 m, b
[411] vw			B_{3g}			-		
[388] vw			B_{1g}			-		
330 w	-	347 m	A_g	-	B_{1u}	429 w	-	465 m, b
		289 s			B_{3u}			395 w
								353 vw?
222 m	-	215 s	B_{2g}	-	B_{3u}	349 w	-	317 m
184 vs			A_g			300 vs		
		166 m			B_{2u}			227 m
		132 w			B_{1u}			160 w
113 m			B_{2g}			255 m		
110 m			B_{3g}			233 m		
		[48] vw			B_{3u}			*)

vs = very strong, s = strong, m = medium, w = weak, vw = very weak, sh = shoulder, b = broad, O_t = terminal oxygen atom, O_{br} = bridging oxygen atom, vw? = very weak peak on the shoulder of a medium peak, ¯ Davydov pairs, *) outside of measurement range. Frequencies in square brackets were not observed in the powder spectra, but have been reported for single crystal spectra.

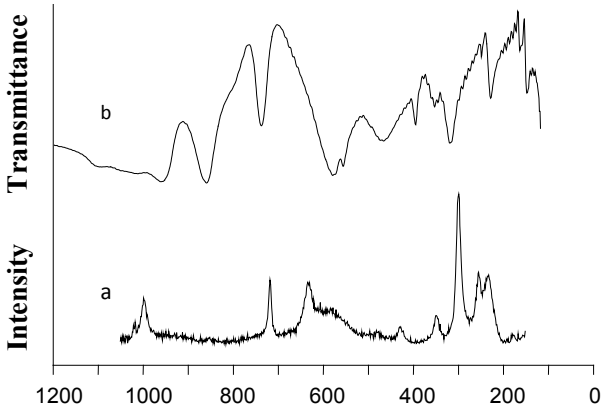

Figure 5. Raman (a) and IR/FIR (b) spectra of $CuSiO_3$ at room temperature.

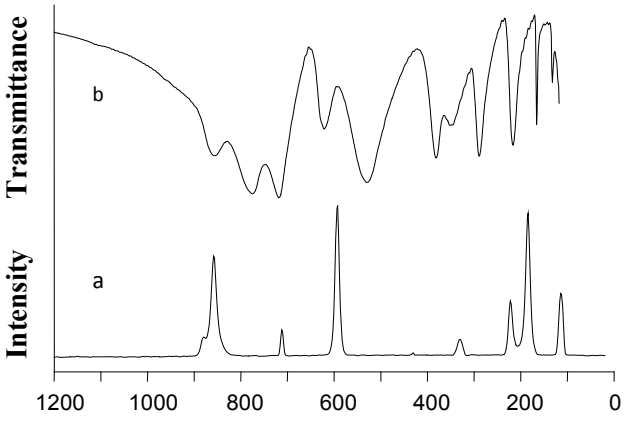

Figure 6. Raman (a) and IR/FIR (b) spectra of $CuGeO_3$ at room temperature.

$F_{m^*} = (m^*_{germanate}/m^*_{silicate})^{1/2} = 1.13$, where m^* is the reduced mass, and $F_{bl} = \langle d\rangle_{germanate}/\langle d\rangle_{silicate} = 1.08$; the mean bond lengths (bl) were applied as a measure of the stiffness of the compounds with $\langle d\rangle = 1.747$ Å for the germanate and $\langle d\rangle = 1.611$ Å for the silicate (**Table 2**).

The frequency quotient of silicate to germanate modes versus the germanate frequency affords some information about the source of the vibrations and is displayed in **Figure 7**. In this drawing three regions of different slope can be made out, beginning with a low frequency region below 250 cm^{-1} (350 cm^{-1} for the silicate) originating from Cu and Ge/Si atom vibrations, then a region between 250 cm^{-1} and 550 cm^{-1} (350 to 600 cm^{-1}) with Cu–O and Ge/Si–O vibrations, and finally the region above 550 cm^{-1} showing modes with a dominant contribution of oxygen vibrations. For the minimum values of the curve it is allowed to neglect F_{m^*} thus obtaining a value, which actually reflects the force constant ratio. In **Figure 7** distinction is also made between Raman and IR data in order to demonstrate the difference of their low frequency modes. Because the copper atom does not contribute to the Raman spectrum (**Table 3**), the large Ge to Si mass ratio is decisive for the large frequency ratio, while for the IR spectrum the contribution of Cu to the reduced mass level out the frequency difference between germanate and silicate.

The number of modes found in the spectra are in agreement with the space group symmetry and f.g.a. taking into account the following points. Three very weak bands in the vibrational spectra of $CuGeO_3$, given in **Table 3** in squares, which have been observed in polarized single crystal spectra [19], are absent in the spectra of powder samples of both $CuGeO_3$ and $CuSiO_3$ due to very low intensity. For the silicate, the peak with the lowest Raman frequency obviously lies outside of the measurement range. A very broad band at 465 cm^{-1} in the IR-spectrum of $CuSiO_3$ is interpreted as a double peak. Two very broad bands in the Raman spectrum of $CuSiO_3$, showing no counterpart in the $CuGeO_3$ spectrum, may be caused by surface effects due to the very small crystallite size, which is concluded from the broad X-ray diffraction peaks observed [10]. Finally, a very weak side band at 353 cm^{-1} observed in the IR spectrum of $CuSiO_3$

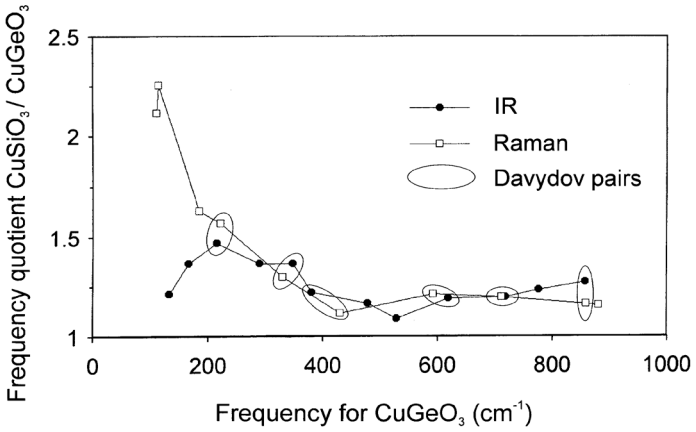

Figure 7. Frequency ratio of silicate to germanate modes versus the germanate frequency. Raman data are depicted as empty squares, IR data as filled circles, respectively. Davydov pairs are indicated by elliptical frames.

may belong to interference fringes caused by the parallelism of the faces of the pressed CsI disk [22].

Once the correct mode assignment has been found, it is sufficient to apply to the silicate the results of the normal coordinate analysis for the germanate, already given by Popović *et al.* [19], in order to find out what the origin of an individual vibration is.

With regard to the crystal symmetry, the spectroscopic data as well as *X*-ray diffraction results are supported by a further experiment. According to NQR measurements of Cu in $CuSiO_3$ there exists, even down to 4.2 K, only one Cu site [25].

Following Popović *et al.* [19], we can analyse the chain mode doublets (Davydov pairs) for $CuSiO_3$, like that for $CuGeO_3$, as the result of the vibration of a pair of weakly coupled identical oscillators by the relation $\nu_{\pm} = (\nu_0^2 \pm \Delta^2)^{1/2}$, where ν_0 is the frequency of the isolated oscillators and Δ^2 is proportional to the coupling force constant. Then $(\nu_0/\Delta)^2$ gives a measure of the ratio of intralayer-to-interlayer bond strength. **Table 4** summarizes the phonon doublet analysis ($\nu_+ = \nu_{Raman}$, $\nu_- = \nu_{IR}$), which yields the mean value of $(\nu_0/\Delta)^2$ for the silicate about 20 % lower than for the germanate [18], in accordance with the changed chain separations that have been derived from the crystal structure analysis (**Table 1**).

The more 3*D*-like character of the silicate may be responsible for the different spin-phonon coupling in comparison to the germanate leading at low temperature to a long-range antiferromagnetic *Néel* state order instead of a spin-*Peierls* order.

6. Conclusions

The vibrational spectra of orthorhombic $CuSiO_3$ from powder samples are presented. The observed Raman respectively IR modes are assigned based on single crystal results for $CuGeO_3$ previously given. A chain mode analysis of *Davydov*

Table 4. Analysis of Raman and infrared active phonon doublets for $CuSiO_3$. Frequencies ν and Δ are given in cm^{-1}.

ν_{Raman}	ν_{IR}	ν_0	Δ	$(\nu_0/\Delta)^2$
A_g	B_{1u}			
429	465*)	447	128	12
719	737	728	115	40
998	1092	1045	313	11
B_{2g}	B_{3u}			
349	317	333	105	10
480	465*)	473	85	31
B_{3g}	B_{2u}			
853	859	856	72	143
		$<(\nu_0/\Delta)^2> =$	41	

*) This broad band is interpreted as a double peak.

pairs suggested that the intralayer-to-interlayer bond strengths for the silicate are about 20% lower than for the germanate, reflecting the different magnetic behaviour of the silicate and the germanate.

Single crystals of $CuSiO_3$ are required to improve the obtained vibration spectra and extend the measurement to low temperatures and to perform a meaningful lattice dynamical calculation. However, the generation of thin $CuSiO_3$ layers may be a promising task [26].

The negligible mismatch between certain lattice parameters of tenorite (CuO) and $CuSiO_3$ suggests the possibility of a metastable formation of $CuSiO_3$ by the way of a topotactically induced reaction on the tenorite surface. It is proposed to use a tenorite substrate or at least a tenorite buffer layer for an epitaxial growth of well crystallized copper polysilicate. Like straw crystals of TiO_2 (rutile) [27] or $CuGeO_3$ nanorods [28], also $CuSiO_3$ may show photocatalytic activity for the degradation of wastewater or toxic NO_x exhaust gases under sun light exposure. Therefore, dd-excitations and the energy gap of $CuSiO_3$ were empirically estimated quite recently, due to the lack of pure crystalline material or even single crystals to experimentally measure the spectra [29] [30].

Acknowledgements

The authors would like to thank the late Prof. Dr. W. Brockner, Institute of Inorganic and Analytical Chemistry at the TU Clausthal, for the opportunity to measure the spectra.

References

[1] Hase, M., Terasaki, I. and Uchinokura, K. (1993) Observation of the Spin-Peierls transition in Linear Cu^{2+} (Spin-1/2) Chains in an Inorganic Compound $CuGeO_3$. *Physical Review Letters*, **70**, 3651-3654. https://doi.org/10.1103/PhysRevLett.70.3651

[2] Boucher, J.P. and Regnault, L.P. (1966) The Inorganic Spin-Peierls Compound $CuGeO_3$. *Journal de Physique I*, **6**, 1939-1966. https://doi.org/10.1051/jp1:1996198

[3] Isobe, M. and Ueda, Y. (1996) Magnetic Susceptibility of Quasi-One-Dimensional α' – NaV_2O_5 – Possible Spin-Peierls Compound with High Critical Temperature of 34K. *Journal of the Physical Society of Japan*, **65**, 1178-1181. https://doi.org/10.1143/JPSJ.65.1178

[4] Ginetti, Y. (1954) Structure cristalline du métagermanate de cuivre. *Bulletin Sociétés Chimiques Belges*, **63**, 209-216. https://doi.org/10.1002/bscb.19540630501

[5] Völlenkle, H., Wittmann, A. and Nowotny, H. (1967) Zur Kristallstruktur von $CuGeO_3$. *Monatshefte für Chemie*, **98**, 1352-1357. https://doi.org/10.1007/BF00909002

[6] Breuer, K.H. (1984) Kristallchemie von Kupfer(II)-Silikaten und -Germanaten. Dissertation Universität Heidelberg.

[7] Liebau, F. (1956) Bemerkungen zur Systematik der Kristallstrukturen von Silikaten mit hochkondensierten Anionen. *Zeitschrift für Physikalische Chemie*, **206**, 73-90. https://doi.org/10.1515/zpch-1956-0107

[8] Dent Glasser, L.S. (1979) Non-Existent Siliocates. *Zeitschrift für Kristallographie*, **149**, 291-305.

[9] Otto, H.H., Brandt, H.J. and Meibohm, M. (1996) Über die Existenz des Kupferpolysilicats $Cu\{uB_1 1_\infty{}^1\}[^1SiO_3]$. *Beihefte zu European Journal of Mineralogy*, **8**, 206.

[10] Otto, H.H. and Meibohm, M. (1999) Crystal Structure of Copper Polysilicate, $Cu[SiO_3]$. *Zeitschrift für Kristallographie*, **214**, 558-565. https://doi.org/10.1524/zkri.1999.214.9.558

[11] Meibohm, M. (1999) Zur Kristallchemie und Kristallphysik von neuen Silikaten und Germanaten des Kupfers mit ketten- und ringförmigen Anionen. Doctoral Thesis, TU Clausthal.

[12] Wolfram, H., Otto, H.H., Cwik, M., Braden, M., André, G., Bourée, G.F., Baenitz, M. and Steglich, F. (2004) Neutron Diffraction Study of the Nuclear and Magnetic Structure of the Quasi-One-Dimensional Compound $CuSiO_3$ around $T_N = 8$ K. *Physical Review B*, **69**, 144115-144127. https://doi.org/10.1103/PhysRevB.69.144115

[13] Braden, M., Wilkendorf, G., Lorenzana, J., Ain, M., McIntyre, G.J., Behruzi, M., Heger, G., Dhalenne, G. and Revcolevschi, A. (1996) Structural Analysis of $CuGeO_3$: Relation between Nuclear Structure and Magnetic Interaction. *Physical Review B*, **54**, 1105-1116. https://doi.org/10.1103/PhysRevB.54.1105

[14] Tanaka, I., Shibuya, Y. and Kojima, H. (1996) Crystal Growth of Pure and Zn-Doped $CuGeO_3$ by the Floating Zone (FZ) Method. *Journal of Crystal Growth*, **169**, 469-473. https://doi.org/10.1016/S0022-0248(96)00447-2

[15] Meibohm, M., Otto, H.H. and Brockner, W. (2009) Vibrational Spectra of Copper Polysilicate, $CuSiO_3$. arXiv e-Print (arXiv:0903.3901).

[16] Rousseau, D.L., Bauman, R.P. and Porto, S.P.S. (1981) Normal Mode Determination in Crystals. *Journal of Raman Spectroscopy*, **10**, 253-290. https://doi.org/10.1002/jrs.1250100152

[17] Adams, D.M. and Newton, D.C. (1970) Tables for Factor Group and Point Group Analysis. Beckman R.I.I.C., Croydon.

[18] Adams, D.M. and Fletcher, P.A. (1988) Vibrational Spectroscopy at High Pressure: Part 53. Alkali Metavanadates and Copper Metagermanate. *Spectrochimica Acta A*, **44**, 233-240.

[19] Popović, Z.V., Dević, S.D., Popov, V.N., Dhalenne, G. and Revcolevschi, A. (1995) Phonons in $CuGeO_3$ Studied Using Polarized Far-Infrared and Raman-Scattering Spectroscopies. *Physical Review B*, **52**, 4185-4190.

https://doi.org/10.1103/PhysRevB.52.4185

[20] Dević, S.D., Konstantinović, M.J., Popović, Z.V., Dhalenne, G. and Revcolevschi, A. (1994) Vibrational Properties of Copper Metagermanate ($CuGeO_3$). *Journal of the Physics of Condensed Matter*, **6**, L745.

[21] Dević, S.D., Popović, Z.V., Popov, V.N., Dhalenne, G. and Revcolevschi, A. (1997) Temperature Dependence of Raman Active Modes in $CuGeO_3$. *Solid State Communications*, **102**, 599-604. https://doi.org/10.1016/S0038-1098(97)00027-6

[22] Kuroe, H., Sekine, T., Hase, M., Sasago, Y., Uchinokura, K., Kojima, H., Tanaka, I. and Shibuya, Y. (1994) Raman-Scattering Study of $CuGeO_3$ in the Spin-Peierls Phase. *Physical Review B*, **50**, 16468-16474. https://doi.org/10.1103/PhysRevB.50.16468

[23] Udagawa, M., Aoki, H., Ogita, N., Fujita, O., Sohma, A., Ogihara, A. and Akimitsu, J. (1994) Raman Scattering of $CuGeO_3$. *Journal of the Physical Society of Japan*, **63**, 4060-4064. https://doi.org/10.1143/JPSJ.63.4060

[24] Davydov, A.S. (1962) Theorie of Molecular Excitations. MacGraw-Hill Book Comp., New York, San Francisco, Toronto, London.

[25] Baenitz, M., Geibel, C., Dischner, M., Sparn, G., Steglich, F., Otto, H.H., Meibohm, M. and Gipius, A.A. (2000) $CuSiO_3$: A Quasi-One-Dimensional S = 1/2 Antiferromagnetic Chain System. *Physical Review B*, **62**, 12201-12205. https://doi.org/10.1103/PhysRevB.62.12201

[26] Otto, H.H. (2016) A Different Approach to High-T_c Superconductivity: Indication of Filamentary-Chaotic Conductance and Possible Routes to Superconductivity above Room Temperature. *World Journal of Condensed Matter Physics*, **6**, 244-260. https://doi.org/10.4236/wjcmp.2016.63023

[27] Li, G., Boerio-Goates, J. and Woodfield, B.F. (2004) Evidence of Linear Lattice Expansion and Covalency Enhancement in Rutile TiO_2 Nanocrystals. *Applied Physics Letters*, **85**, 2059. https://doi.org/10.1063/1.1790596

[28] Borhade, A.V., Gaikwad, V.B., Baste, Y.R. and Tope, D.R. (2013) Synthesis and Characterization of $CuGeO_3$ Photocatalyst Using Green Chemistry and Its Application for the Degradation of Direct Black Dye. *Carbon—Science and Technology*, **5**, 192-196.

[29] Otto, H.H. (2018) $CuSiO_3$: Empirical Estimation of dd-Excitations and the Energy Gap.

[30] Otto, H.H. (2017) Crystal Growth of $Cu_6(Ge,Si)_6O_{18}\cdot 6H_2O$ and Assignment of UV-VIS Spectra in Comparison to Dehydrated Dioptase and Selected Cu(II) Oxo-Compounds Including Cuprates. *World Journal of Condensed Matter Physics*, **7**, 57-79. https://doi.org/10.4236/wjcmp.2017.73006